Feeding state sculpts a circuit for sensory valence in *Caenorhabditis elegans*

Sophie Rengarajan[a], Kristen A. Yankura[a], Manon L. Guillermin[a], Wendy Fung[a], and Elissa A. Hallem[a,1]

[a]Department of Microbiology, Immunology, and Molecular Genetics, University of California, Los Angeles, CA 90095

Edited by H. Robert Horvitz, Massachusetts Institute of Technology, Cambridge, MA, and approved December 12, 2018 (received for review May 1, 2018)

Hunger affects the behavioral choices of all animals, and many chemosensory stimuli can be either attractive or repulsive depending on an animal's hunger state. Although hunger-induced behavioral changes are well documented, the molecular and cellular mechanisms by which hunger modulates neural circuit function to generate changes in chemosensory valence are poorly understood. Here, we use the CO_2 response of the free-living nematode *Caenorhabditis elegans* to elucidate how hunger alters valence. We show that CO_2 response valence shifts from aversion to attraction during starvation, a change that is mediated by two pairs of interneurons in the CO_2 circuit, AIY and RIG. The transition from aversion to attraction is regulated by biogenic amine signaling. Dopamine promotes CO_2 repulsion in well-fed animals, whereas octopamine promotes CO_2 attraction in starved animals. Biogenic amines also regulate the temporal dynamics of the shift from aversion to attraction such that animals lacking octopamine show a delayed shift to attraction. Biogenic amine signaling regulates CO_2 response valence by modulating the CO_2-evoked activity of AIY and RIG. Our results illuminate a new role for biogenic amine signaling in regulating chemosensory valence as a function of hunger state.

C. elegans | carbon dioxide | sensory valence | biogenic amines | starvation

To appropriately respond to their environments, animals must detect external chemosensory stimuli and respond to these stimuli in the context of their internal needs. The integration of external stimuli with internal state establishes a framework for ethologically relevant behavior. A critical aspect of an animal's internal state is its hunger state. The responses to many chemosensory cues depend on hunger state (1), and some chemosensory cues can be either appetitive or aversive as a function of hunger (2). For example, humans perceive some food-associated odors as appetitive only when hungry (3, 4). However, little is known about the molecular and cellular mechanisms that modulate neural circuit function to generate feeding-state-dependent changes in the valence of a chemosensory stimulus. *Caenorhabditis elegans* is a powerful genetic model for elucidating the molecular and cellular mechanisms that regulate chemosensory behaviors as a function of feeding state. Despite its small nervous system, *C. elegans* exhibits complex behavioral responses to a wide range of chemosensory stimuli, and many of these responses are altered by changes in feeding state (5, 6). Moreover, *C. elegans* has an extensive genetic toolkit and is easily amenable to quantitative behavioral analysis (6). Thus, *C. elegans* is a uniquely tractable system for addressing how chemosensory circuits are modulated by feeding state.

One of the sensory behaviors of *C. elegans* that can be modulated by feeding state is the response to carbon dioxide (CO_2). CO_2 is an ambiguous sensory stimulus for *C. elegans* that can signal either favorable environments, such as bacterial food or mates, or unfavorable environments, such as predators, pathogens, or overcrowding (6–8). Consistent with this ambiguity, CO_2 can be attractive, repulsive, or neutral for *C. elegans* depending on its life stage, recent experience, and internal state (6, 9–15). For example, well-fed *C. elegans* adults are repelled by CO_2 when raised at ambient CO_2 (~0.038%), but are attracted to CO_2 when raised in a high-CO_2 environment (2.5%) (14). In addition, while well-fed animals raised at ambient CO_2 are repelled by it, starved animals raised at ambient CO_2 no longer exhibit repulsion (9, 10). At the cellular level, CO_2 chemotaxis is mediated primarily by the BAG sensory neurons, although other sensory neurons also contribute (9, 11, 16–18). Four pairs of interneurons—AIY, AIZ, RIA, and RIG—operate downstream of BAGs to mediate CO_2 response (13, 14).

Here, we show that hunger alters CO_2 response valence. Food deprivation results in a gradual shift from CO_2 repulsion to CO_2 attraction, and this shift is reversed upon refeeding. At the circuit level, this transition is mediated by a change in the CO_2-evoked activity of RIG and AIY. At the molecular level, it is mediated by opposing biogenic amine signals. Our results identify a role for biogenic amines in regulating chemosensory valence as a function of hunger state.

Results

CO_2 Response Valence Changes During Starvation. Whereas well-fed *C. elegans* adults previously had been found to avoid CO_2 (9–12, 16), we found that starved adults are attracted to CO_2 in a chemotaxis assay (Fig. 1*A* and *SI Appendix*, Fig. S1). Refeeding starved animals restores CO_2 avoidance (Fig. 1*A*). The response of *C. elegans* to CO_2 therefore provides a system for understanding the mechanisms by which hunger regulates chemosensory valence. We first investigated how hunger shapes the behavioral response to CO_2 by comparing CO_2-evoked behavior in animals deprived of food for varying lengths of time. We found that CO_2 response valence shifts over the course of hours during starvation (Fig. 1*B*). CO_2 attraction in starved animals was observed across a wide range of CO_2 concentrations (Fig. 1*C*). Thus, the change in CO_2

Significance

Hunger regulates many animal behaviors. In particular, some chemosensory stimuli can be attractive or repulsive depending on the feeding state of an animal. The neural basis for hunger-dependent changes in chemosensory valence is poorly understood. Here, we show that the response of *Caenorhabditis elegans* to CO_2 depends on hunger. CO_2 shifts from repulsive to attractive during starvation. This valence change results from modulation of the CO_2 circuit by opposing biogenic amine signals. Dopamine promotes repulsion in well-fed animals, whereas octopamine promotes attraction in starved animals. Biogenic amine signaling alters the CO_2-evoked activity of interneurons in the CO_2 circuit, resulting in hunger-dependent changes in CO_2 response valence. Our results illustrate a role for biogenic amine signaling in determining chemosensory valence.

Author contributions: S.R., K.A.Y., M.L.G., W.F., and E.A.H. designed research; S.R., K.A.Y., M.L.G., and W.F. performed research; S.R., K.A.Y., M.L.G., W.F., and E.A.H. analyzed data; and S.R. and E.A.H. wrote the paper.

The authors declare no conflict of interest.

This article is a PNAS Direct Submission.

[1]To whom correspondence should be addressed. Email: ehallem@ucla.edu.

This article contains supporting information online at www.pnas.org/lookup/suppl/doi:10.1073/pnas.1807454116/-/DCSupplemental.

Published online January 16, 2019.

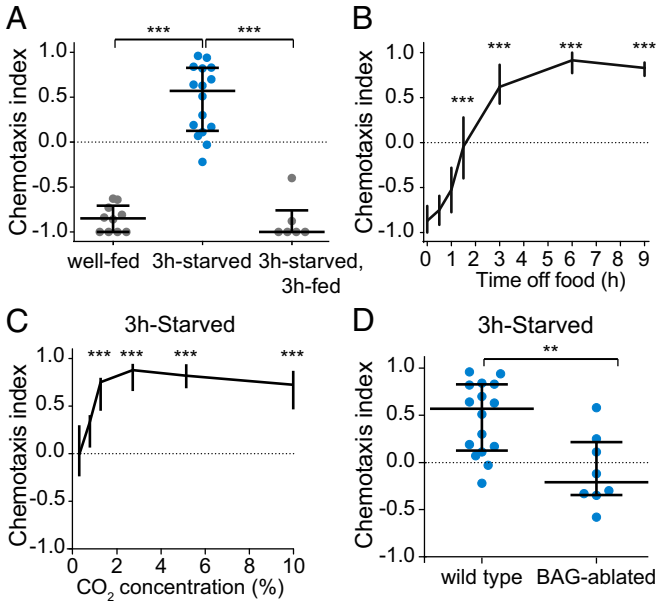

Fig. 1. CO_2 response valence shifts during starvation. (*A*) Well-fed animals are repelled by CO_2, and 3-h-starved animals are attracted to CO_2. Refeeding 3-h-starved animals for 3 h restores CO_2 repulsion. n = 6–16 trials per condition. ***P < 0.001, Kruskal–Wallis test with Dunn's posttest. (*B*) CO_2 response valence shifts from repulsion to attraction over the course of 3 h. n = 10–70 trials per condition. ***P < 0.001, Kruskal–Wallis test with Dunn's posttest. (*C*) 3-h-starved animals are attracted to CO_2 across a wide range of concentrations. n = 6–16 trials per condition. ***P < 0.001, Kruskal–Wallis test with Dunn's posttest. (*D*) 3-h-starved BAG-ablated animals do not respond to CO_2, indicating that BAG is required for CO_2 attraction. n = 8–16 trials per genotype. **P < 0.01, Mann–Whitney U test. Responses are to 10% CO_2 except where concentrations are indicated (*C*).

response valence induced by hunger is reversible and relatively concentration-independent.

CO_2 Circuit Interneuron Activity Is Modulated by Starvation. We then asked how starvation modulates the CO_2 microcircuit. Starvation could regulate valence by acting on the sensory neurons at the level of CO_2 detection, or it could act downstream at the level of interneurons or motor neurons. To determine where feeding state is first integrated in the CO_2 microcircuit, we tested whether starvation modulates the activity of the CO_2-detecting BAG neurons. BAG previously had been shown to be required for both avoidance and attraction in the context of well-fed animals cultivated in high- and low-CO_2 environments (14). We found that starved animals lacking BAG do not respond to CO_2 (Fig. 1*D*), indicating that BAG is required for CO_2 attraction in starved animals. We then examined the CO_2-evoked activity of BAG and found that it is similar in well-fed and starved animals (*SI Appendix*, Fig. S2). Thus, starvation regulates CO_2 response downstream of the BAG calcium response.

We next examined whether starvation regulates CO_2 response by modulating the activity of interneurons directly downstream of BAG. CO_2 response is mediated by four interneuron pairs downstream of BAG: AIY, AIZ, RIA, and RIG (13, 14). Three of these pairs—AIY, RIA, and RIG—regulate CO_2 response valence in animals raised at high vs. low CO_2 (14). To determine whether the same interneurons regulate CO_2 response during starvation, we screened strains in which each pair of interneurons was genetically ablated (14). We found that two of these interneuron pairs, RIG and AIY, regulate CO_2 response during starvation. Whereas wild-type animals were neutral to CO_2 after 1.5 h of food deprivation, RIG-ablated animals were attracted to CO_2 (*SI Appendix*, Fig. S3). Thus, RIG promotes CO_2 avoidance during the early stages of food deprivation. In contrast, AIY-ablated animals failed to shift to CO_2 attraction after 6 h of food deprivation, suggesting that AIY promotes attraction during starvation (*SI Appendix*, Fig. S3). Together, these results suggest that RIG and AIY act antagonistically and on different timescales to regulate CO_2 response as a function of feeding state. However, AIY ablation is known to alter navigation behavior in other contexts (19, 20), and general navigation deficits may contribute to changes in CO_2 chemotaxis during starvation. RIA-ablated animals showed a normal shift to CO_2 attraction during starvation, suggesting that RIA is not required for starvation-dependent modulation of CO_2 response (*SI Appendix*, Fig. S3).

To determine how RIG and AIY regulate CO_2 response during starvation, we monitored their CO_2-evoked activity in well-fed and starved animals. RIG showed CO_2-evoked excitatory responses in well-fed but not in 6-h-starved animals; 1.5-h-starved animals showed an intermediate response or no response (Fig. 2). In the case of AIY, well-fed animals showed consistently inhibitory responses to CO_2 but starved animals showed two categorically different responses to CO_2: excitatory and inhibitory (Fig. 3). The responses of AIY in starved animals are probabilistic, such that excitatory and inhibitory responses were observed with approximately equal frequency (Fig. 3). CO_2-evoked excitatory responses in AIY previously had been shown to promote CO_2 attraction in a different context (14), suggesting that the excitatory activity of AIY during starvation promotes CO_2 attraction. Together, our calcium imaging and behavioral

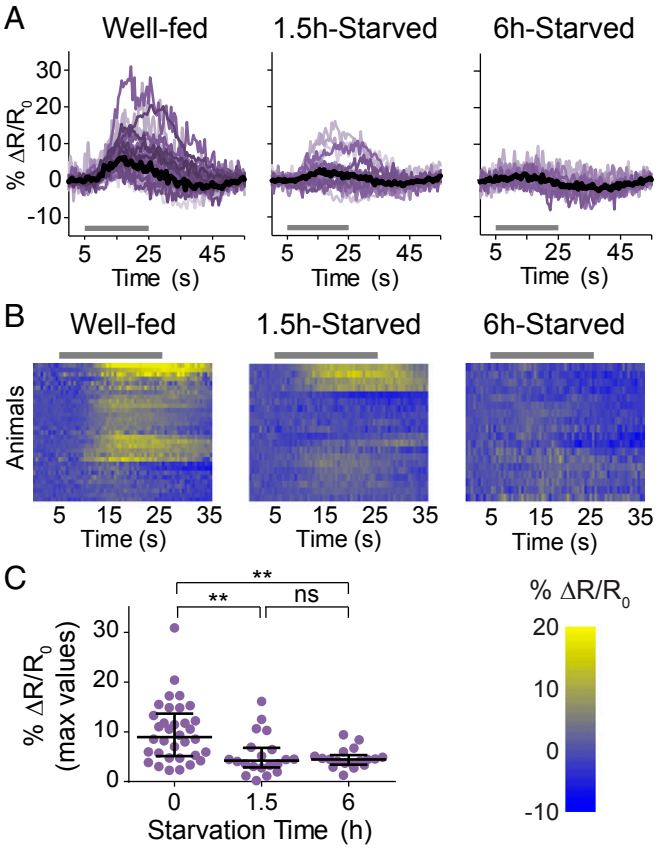

Fig. 2. Starvation suppresses the CO_2-evoked activity of RIG. (*A*) Colored lines depict individual traces, and black lines depict medians. (*B*) Each row represents the response of an individual animal. Responses are ordered by hierarchical cluster analysis. (*A* and *B*) Gray bars indicate the timing of the CO_2 pulse. (*C*) The dot plot shows maximum values of % $\Delta R/R_0$ for each animal; lines show medians and interquartile ranges. n = 17–18 animals per condition. **P < 0.01, Kruskal–Wallis test with Dunn's posttest. Responses are to 10% CO_2.

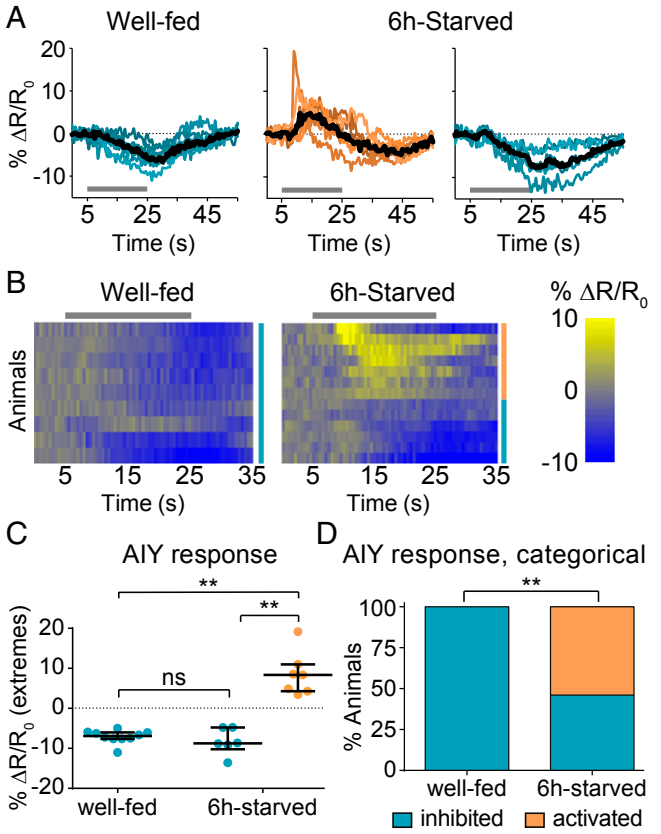

Fig. 3. Starvation results in probabilistic CO_2-evoked activity in AIY. AIY shows inhibitory responses in well-fed animals but both excitatory and inhibitory responses in 6-h-starved animals. (*A*) Colored lines depict individual traces, and black lines depict medians. (*B*) Each row represents the response of an individual animal. Responses are ordered by hierarchical cluster analysis; orange and blue coding indicates excitatory and inhibitory responses, respectively. (*A* and *B*) Gray bars indicate the timing of the CO_2 pulse. (*C*) The dot plot shows maximum values (for excitatory responses) or minimum values (for inhibitory responses) of % $\Delta R/R_0$ for each animal; lines show medians and interquartile ranges. (*D*) The categorical plot depicts the percentage of excitatory and inhibitory responses. $n = 9$–13 animals per condition. $^{**}P < 0.01$, Kruskal–Wallis test with Dunn's posttest (*C*) or Fisher's exact test (*D*). ns, not significant. Responses are to 15% CO_2.

data suggest that the excitatory activity of RIG promotes CO_2 repulsion in well-fed animals and regulates the timing of the valence switch, whereas the probabilistic CO_2-evoked excitatory activity of AIY promotes CO_2 attraction during starvation. Thus, starvation regulates the CO_2 circuit at least in part by modulating interneuron activity.

AIY Calcium Activity Reflects Behavioral Robustness. Like starved animals, animals raised with food in a high-CO_2 environment are attracted to CO_2 (14). However, a direct comparison of CO_2 attraction in these two sets of animals revealed that CO_2-cultivated animals show more extreme CO_2 attraction than do starved animals (*SI Appendix*, Fig. S4 *A* and *B*). While both groups of animals migrated toward CO_2, CO_2-cultivated animals gathered directly under the CO_2 source (*SI Appendix*, Fig. S4*A*). Thus, the CO_2 attraction of starved animals represents a less extreme behavioral state than that of animals cultivated with food at high CO_2. This behavioral difference may reflect a risk-benefit calculation in starved worms, as they weigh the ethological ambiguity of a CO_2 stimulus with the uncertainty of food availability. This ambiguity is not faced by worms cultivated at high CO_2 in the presence of food. In these animals, the positive association between a high-CO_2 environment and food may result in stronger attraction. To investigate the neural mechanisms that underlie these differences in behavioral sensitivity to CO_2, we compared the CO_2-evoked activity of AIY in starved vs. CO_2-cultivated animals. While starved animals raised at ambient CO_2 showed a roughly equal proportion of excitatory and inhibitory responses in AIY, well-fed animals raised at high CO_2 showed primarily excitatory responses (*SI Appendix*, Fig. S4 *C*–*E*) (14). In addition, the excitatory responses of AIY in CO_2-cultivated animals were larger than those in starved animals (*SI Appendix*, Fig. S4 *D* and *E*). Thus, the decreased variability and increased amplitude of AIY responses correlate with increased behavioral robustness. These results suggest that AIY activity may control behavioral sensitivity to CO_2.

Dopamine Promotes CO_2 Avoidance in Well-Fed Animals. We next investigated the neuromodulatory mechanisms that regulate CO_2 response valence as a function of feeding state. Across species, many hunger-dependent changes in sensory behavior are mediated by biogenic amines (1, 21). In *C. elegans*, biogenic amines play important roles in signaling the presence or absence of food (1, 21). We therefore investigated whether biogenic amine signaling regulates CO_2 response across feeding states. We first explored a potential role for dopamine by assaying the CO_2-evoked behavior of *dat-1::ICE* animals, which contain a genetic ablation of dopaminergic neurons due to expression of the human caspase ICE under the control of the promoter for the

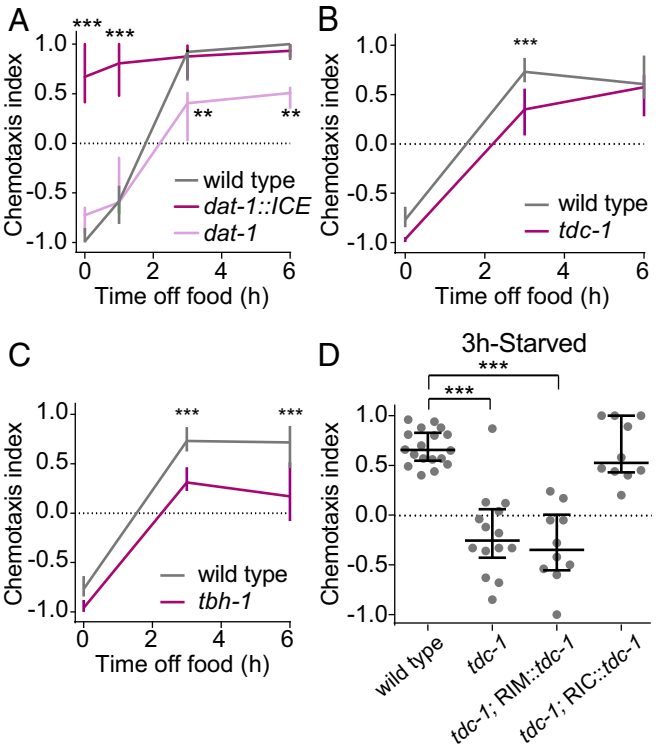

Fig. 4. Biogenic amine signaling regulates CO_2 response valence during starvation. (*A*) Dopamine promotes CO_2 avoidance. Wild-type, *dat-1::ICE*, and *dat-1* animals were food-deprived for 0–6 h. $n = 8$–14 trials per genotype and condition. $^{**}P < 0.01$ and $^{***}P < 0.001$, two-way ANOVA with Sidak's posttest. (*B* and *C*) Octopamine signaling promotes CO_2 attraction. Loss of both tyramine and octopamine signaling (*B*) or only octopamine signaling (*C*) delays the shift to CO_2 attraction. Wild-type, *tdc-1*, or *tbh-1* animals were food-deprived for 0–6 h. $n = 6$–14 trials per genotype and condition. $^{***}P < 0.001$, two-way ANOVA with Sidak's posttest. (*D*) Restoring *tdc-1* function to 3-h-starved *tdc-1* mutants in octopaminergic RIC neurons but not in tyraminergic RIM neurons restores CO_2 attraction. $n = 10$–18 trials per genotype. $^{***}P < 0.001$, one-way ANOVA with Dunnett's posttest. For all graphs, lines show medians and interquartile ranges. Responses are to 10% CO_2.

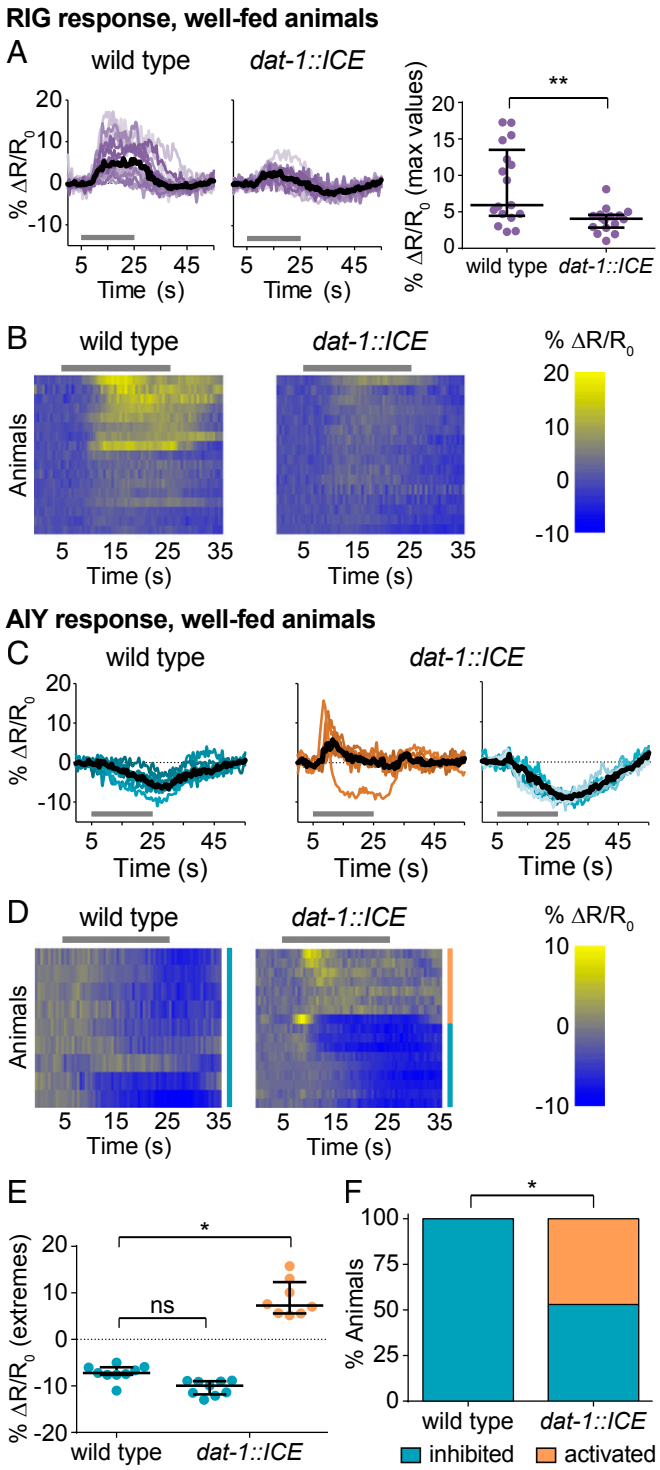

Fig. 5. Dopaminergic signaling acts on RIG and AIY to promote CO_2 avoidance. (*A* and *B*) The CO_2-evoked activity of RIG is attenuated in well-fed *dat-1::ICE* animals compared with wild-type animals. n = 16–17 animals per genotype. $^{**}P < 0.01$, unpaired Student's t test with Welch's correction. (*C*–*F*) Well-fed *dat-1::ICE* animals show more excitatory and fewer inhibitory CO_2-evoked responses in AIY compared with well-fed wild-type animals. n = 9–17 animals per genotype. $^{*}P < 0.05$, Kruskal–Wallis test with Dunn's posttest (*E*) or χ^2 test (*F*). (*A* and *C*) Colored lines depict individual traces, and black lines depict medians. (*B* and *D*) Each row represents the response of an individual animal. Responses are ordered by hierarchical cluster analysis. (*D*) Orange and blue coding indicates excitatory and inhibitory responses, respectively. (*A*–*D*) Gray bars indicate the timing of the CO_2 pulse. Dot plots depict maximum (for *A* and excitatory responses in *E*) or minimum (for inhibitory responses in *E*) values of % $\Delta R/R_0$ for each animal. Lines in dot plots show medians and interquartile ranges. Data for wild-type animals (*C*) are also shown in Fig. 3. Responses are to 10% (*A* and *B*) or 15% (*C*–*F*) CO_2.

dopamine transporter gene *dat-1* (22, 23). We found that these animals are attracted to CO_2 regardless of feeding state (Fig. 4*A*). In contrast, starved animals with increased dopamine signaling resulting from loss of the *dat-1* gene (23) showed reduced attraction (Fig. 4*A*). These results suggest that dopaminergic signaling promotes CO_2 avoidance in well-fed animals. To further confirm that dopamine drives CO_2 avoidance, we administered dopamine exogenously to animals for 30 min before assaying their CO_2 response. We found that dopamine treatment restored CO_2 avoidance in *dat-1::ICE* animals (*SI Appendix*, Fig. S5*A*). In addition, dopamine treatment eliminated CO_2 attraction in wild-type animals deprived of food for 3 h, although it did not result in CO_2 avoidance (*SI Appendix*, Fig. S5*B*). Thus, dopamine regulates CO_2 response valence by promoting CO_2 avoidance in well-fed animals. We then screened well-fed animals lacking individual dopamine receptors (21, 24) in a CO_2 chemotaxis assay. However, these mutants responded normally to CO_2 (*SI Appendix*, Fig. S6), suggesting that multiple dopamine receptors act redundantly to regulate CO_2 response.

Octopamine Promotes CO_2 Attraction in Starved Animals. We next investigated the roles of tyramine and octopamine in regulating CO_2 response. Tyramine and octopamine are invertebrate neurotransmitters that are analogous to vertebrate epinephrine and norepinephrine, respectively (25). Animals lacking the tyrosine decarboxylase gene *tdc-1*, which is required for both tyraminergic and octopaminergic signaling, showed a delayed shift from CO_2 avoidance to attraction during starvation (Fig. 4*B*). We then tested animals lacking the tyramine β-hydroxylase gene *tbh-1*, which is required for the conversion of tyramine into octopamine. The *tbh-1* mutants showed a delayed shift to attraction (Fig. 4*C*), demonstrating a specific role for octopamine in promoting CO_2 attraction. Within the nervous system, *tdc-1* is expressed in the RIM motor neurons and the RIC interneurons, while *tbh-1* is expressed only in the RIC interneurons (21). Thus, RIM is tyraminergic and RIC is octopaminergic. To further confirm a role for octopamine in regulating CO_2 response, we performed a rescue experiment in which *tdc-1* function was restored to *tdc-1* mutants in either RIM or RIC (26). Restoring *tdc-1* function in RIC but not RIM was sufficient to restore normal CO_2 attraction in starved animals (Fig. 4*D*). Thus, CO_2 response in starved animals is primarily regulated by octopamine, although we cannot exclude a secondary or redundant role for tyramine. Transiently silencing *tdc-1*-expressing neurons in adult animals using the histamine-gated chloride channel HisCl1 (26, 27) resulted in reduced CO_2 attraction in starved animals (*SI Appendix*, Fig. S7), suggesting that the effects of octopamine on CO_2 response result from real-time modulation of the CO_2 circuit. These results suggest that CO_2 response valence is regulated by opposing biogenic amines. In well-fed animals, dopamine signaling drives CO_2 repulsion; in starved animals, octopamine signaling drives CO_2 attraction.

C. elegans has three octopamine receptors: *ser-3*, *ser-6*, and *octr-1* (21). The *ser-6* mutants, but not the *ser-3* or *octr-1* mutants, showed reduced CO_2 attraction when starved (*SI Appendix*, Fig. S8*A*). The *ser-6* gene is expressed in a subset of head neurons, including the AWB olfactory neurons and the SIA interneurons (28, 29). We found that restoring *ser-6* function to *ser-6* mutants either in all *ser-6*-expressing neurons, in AWB only, or in SIA only was sufficient to restore normal CO_2 attraction to starved animals (*SI Appendix*, Fig. S8 *B* and *C*). These results suggest that SER-6 can function in multiple head neurons to regulate CO_2 response, perhaps through secretion of a shared neuropeptide from these neurons that acts extrasynaptically on the CO_2 circuit.

NEUROSCIENCE

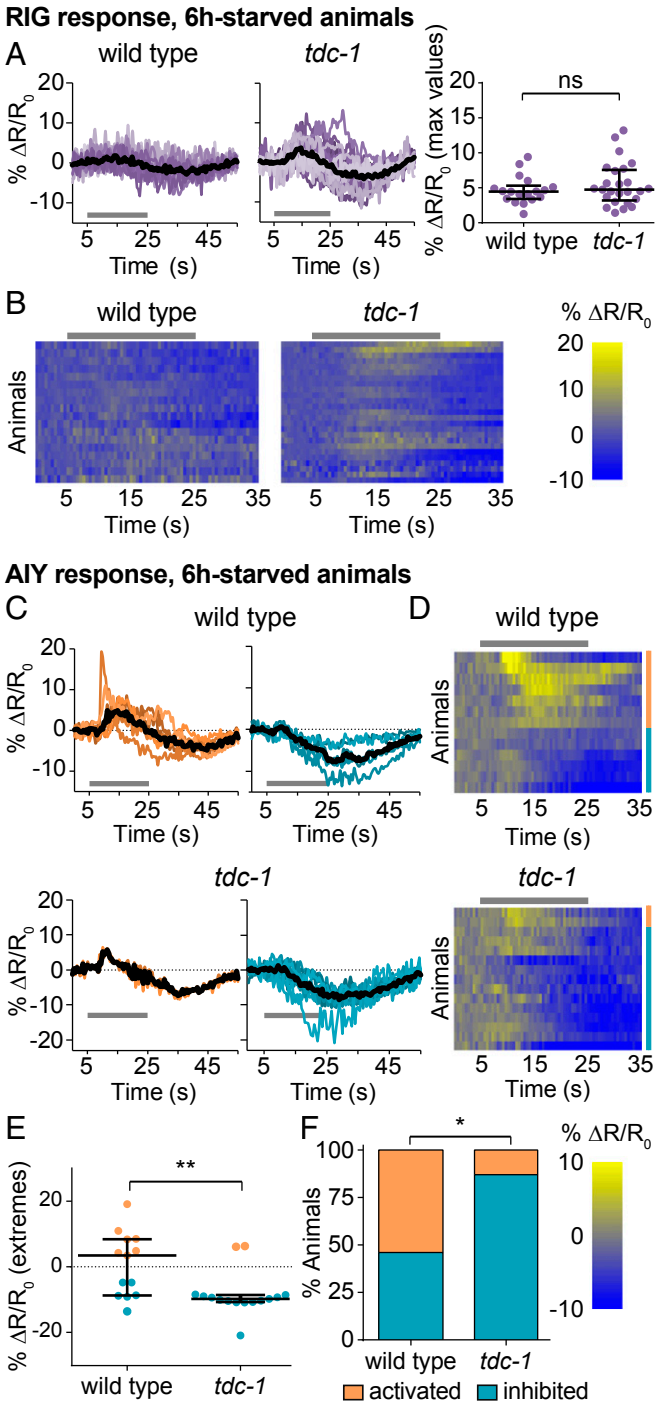

Fig. 6. Octopaminergic signaling acts on AIY but not RIG to promote CO_2 attraction. (*A* and *B*) CO_2-evoked activity in RIG is suppressed in 6-h-starved wild-type and *tdc-1* animals. ns, not significant ($P = 0.4870$), Mann–Whitney *U* test. $n = 18$–25 animals per genotype. (*C*–*F*) 6-h-starved *tdc-1* animals show more inhibitory and fewer excitatory CO_2-evoked responses in AIY than 6-h-starved wild-type animals. $n = 13$–15 animals per genotype. $^*P < 0.05$, $^{**}P < 0.01$, Mann–Whitney *U* test (*E*) or χ^2 test (*F*). (*A* and *C*) Colored lines depict individual traces, and black lines depict medians. (*B* and *D*) Each row represents the response of an individual animal. Responses are ordered by hierarchical cluster analysis. (*D*) Orange and blue coding indicates excitatory and inhibitory responses, respectively. (*A*–*D*) Gray bars indicate the timing of the CO_2 pulse. Dot plots show maximum (for *A* and excitatory responses in *E*) or minimum (for inhibitory responses in *E*) values of % $\Delta R/R_0$ for each animal; lines in dot plots show medians and interquartile ranges. Data for wild-type animals (*A*) are also shown in Fig. 2; data for wild-type animals (*C*) are also shown in Fig. 3. Responses are to 10% (*A* and *B*) or 15% (*C*–*F*) CO_2.

Biogenic Amine Signaling Modulates Interneuron Activity. We next asked how biogenic amine signaling acts on the CO_2 circuit to regulate CO_2 response valence. We first examined how dopamine modulates the CO_2 circuit in well-fed animals to promote CO_2 avoidance. The BAG neurons of well-fed wild-type and *dat-1::ICE* animals showed similar CO_2-evoked activity (*SI Appendix*, Fig. S9 *A* and *B*). In contrast, the CO_2-evoked activity of RIG was decreased in well-fed *dat-1::ICE* animals relative to wild-type animals, suggesting that dopamine enhances the excitatory response of RIG to CO_2 (Fig. 5 *A* and *B*). In addition, AIY in well-fed *dat-1::ICE* animals showed a decreased frequency of inhibitory responses and an increased frequency of excitatory responses, suggesting that dopamine promotes an inhibitory response in AIY (Fig. 5 *C*–*F*). These results suggest that dopamine promotes CO_2 avoidance by modulating interneuron activity. Loss of dopaminergic signaling causes the CO_2-evoked responses of interneurons in well-fed animals to more closely resemble those in starved animals, suggesting that decreased dopaminergic signaling during starvation promotes the shift from CO_2 avoidance to CO_2 attraction.

We then asked how octopamine modulates the CO_2 circuit in starved animals to promote CO_2 attraction. We found that octopamine, like dopamine, regulates the CO_2 circuit downstream of CO_2 detection by BAG (*SI Appendix*, Fig. S9 *C* and *D*). In addition, the RIG neurons of starved *tdc-1* animals resembled those of starved wild-type animals in that they did not show CO_2-evoked activity (Fig. 6 *A* and *B*). In contrast, the AIY neurons of starved *tdc-1* animals showed predominantly inhibitory responses, suggesting that octopamine promotes an excitatory response in AIY (Fig. 6 *C*–*F*). These results suggest that octopaminergic signaling promotes CO_2 attraction by modulating AIY activity, loss of octopamine causes the CO_2-evoked responses of AIY in starved animals to more closely resemble those of well-fed animals, and increased octopaminergic signaling during starvation promotes the shift from CO_2 avoidance to CO_2 attraction.

We previously showed that CO_2 response valence is also regulated by neuropeptide signaling (14). NLP-1 dampens CO_2 repulsion in animals cultivated under low-CO_2 conditions, whereas FLP-16 dampens CO_2 attraction in animals cultivated under high-CO_2 conditions (14). We found that these neuropeptides also regulate CO_2 response valence during starvation: both *nlp-1* and *flp-16* mutants showed a slightly delayed shift from repulsion to attraction during starvation (*SI Appendix*, Fig. S10). Thus, neuropeptide signaling appears to act in concert with biogenic amine signaling to regulate CO_2 response valence. The mechanisms by which neuropeptide signaling modulates CO_2 circuit function remain to be determined.

Discussion

We have demonstrated that CO_2 response valence is modulated by hunger such that the behavioral response to CO_2 shifts from avoidance to attraction during starvation. This shift may reflect an internal risk-benefit analysis. *C. elegans* feeds on aerobic bacteria, which emit CO_2 (30); thus, CO_2 may indicate the presence of a food source. At the same time, both pathogens (8) and predators (31, 32) emit CO_2, making CO_2 an ambiguous and inherently risky sensory cue. Starvation often occurs during periods of environmental uncertainty, when *C. elegans* must forage for food at the expense of encountering predators and pathogens. CO_2 response valence may shift during food deprivation as animals prioritize food seeking over predator evasion. Increased risk taking during starvation has been observed in many animals, including humans (33–37). Thus, hunger regulates risk-taking behaviors across animal phyla.

We have shown that starvation modulates the CO_2 circuit by altering the CO_2-evoked activity of RIG and AIY. RIG shows CO_2-evoked excitatory responses in well-fed animals, but this activity is suppressed during starvation (Fig. 2). In contrast, AIY shows probabilistic CO_2-evoked responses, and starvation state determines the distribution of these responses (Fig. 3). AIY responses in well-fed animals are inhibitory; those in starved animals are both excitatory and inhibitory, with excitatory and inhibitory

responses occurring at roughly equal frequencies (Fig. 3). These results suggest that the increased frequency of AIY excitatory responses promotes CO_2 attraction during starvation.

A comparison of the functional state of the CO_2 circuit in starved animals raised at ambient CO_2 versus well-fed animals raised at high CO_2 (14) demonstrated that, although both sets of animals are attracted to CO_2, well-fed animals at high CO_2 show more extreme CO_2 attraction (*SI Appendix*, Fig. S4 *A* and *B*). The reduced behavioral robustness seen in the starved population may be a mechanism for counterbalancing increased risk taking in an uncertain environment by ensuring that some members of the population survive. Furthermore, the CO_2-evoked activity of AIY differs in the two cases. Starved animals raised at ambient CO_2 show probabilistic AIY responses that can be either excitatory or inhibitory, while well-fed animals raised at high CO_2 show consistent excitatory responses (*SI Appendix*, Fig. S4*C*) (14). Thus, behavioral robustness correlates with the probabilistic activity of AIY. Probabilistic AIY activity has also been observed in response to thermal stimuli and found to correlate with behavioral drive (38), suggesting that AIY may play a similar role in regulating behavior across sensory modalities.

We have shown that different biogenic amines play opposing roles in regulating CO_2 response during starvation. Dopamine promotes avoidance in well-fed animals, while octopamine promotes attraction in starved animals (Fig. 4). Both dopamine and octopamine regulate CO_2 response valence by modulating interneuron activity (*SI Appendix*, Fig. S11). Dopamine modulates the activity of both RIG and AIY (Fig. 5 and *SI Appendix*, Fig. S11), whereas octopamine modulates the activity of AIY but not RIG (Fig. 6 and *SI Appendix*, Fig. S11). Whether the biogenic amines act directly on RIG and AIY, or indirectly on other neurons that modulate RIG and AIY activity, remains to be determined. Neuropeptide signaling also regulates CO_2 response during starvation (*SI Appendix*, Fig. S10), but whether neuropeptide signaling similarly alters RIG and AIY activity remains to be determined as well. Finally, other neurons not tested here may also contribute to changes in the CO_2 circuit during starvation.

In summary, we have demonstrated a role for biogenic amine signaling in regulating chemosensory valence during starvation. All animals navigate through rapidly changing environments, and neural circuits must be dynamically sculpted by current internal state to drive appropriate behaviors. Thus, similar mechanisms of circuit modulation may operate in other organisms to drive internal-state-dependent changes in chemosensory valence.

Materials and Methods

CO_2 chemotaxis assays and calcium imaging were performed as previously described (14). Statistical analysis was performed using GraphPad Prism Version 6.07. For detailed information on all methods, see *SI Appendix, Materials and Methods*.

ACKNOWLEDGMENTS. We thank C. Bargmann (Rockefeller University, New York), M. de Bono (MRC Laboratory of Molecular Biology, Cambridge, United Kingdom), A. Maricq (University of Utah, Salt Lake City), I. Mori (Nagoya University, Nagoya, Japan), S. Mitani (Tokyo Women's Medical University, Tokyo), S. Srinivasan (The Scripps Research Institute, La Jolla, CA), S. Suo (University of Tokyo, Tokyo), and the *Caenorhabditis* Genetics Center for *C. elegans* strains. We also thank Navonil Banerjee, Astra Bryant, Albert Kao, and Jesse Marshall for insightful comments on the manuscript. This work was supported by UCLA-Caltech Medical Scientist Training Program Grant T32GM008042, UCLA Neural Microcircuit Training Grant T32NS058280, and NIH NIGMS F30 Predoctoral Training Grant 1F30GM116810 (to S.R.); an Undergraduate Research Fellowship (Edith and Lew Wasserman Fund for Undergraduate Support) (to W.F.); NSF Graduate Research Fellowship DGE-1144087 and UCLA Cellular and Molecular Biology Training Grant GM007185 (to M.L.G.); and NSF Division of Integrative Organismal Systems Grant IOS-1456064, a McKnight Scholar Award, and an HHMI Faculty Scholar Award (to E.A.H.).

1. Sengupta P (2013) The belly rules the nose: Feeding state-dependent modulation of peripheral chemosensory responses. *Curr Opin Neurobiol* 23:68–75.
2. Li Q, Liberles SD (2015) Aversion and attraction through olfaction. *Curr Biol* 25: R120–R129.
3. O'Doherty J, et al. (2000) Sensory-specific satiety-related olfactory activation of the human orbitofrontal cortex. *Neuroreport* 11:893–897.
4. Smeets PA, et al. (2006) Effect of satiety on brain activation during chocolate tasting in men and women. *Am J Clin Nutr* 83:1297–1305.
5. Bargmann CI (2006) Chemosensation in *C. elegans*. *WormBook*, pp 1–29. Available at www.wormbook.org. Accessed December 1, 2018.
6. Rengarajan S, Hallem EA (2016) Olfactory circuits and behaviors of nematodes. *Curr Opin Neurobiol* 41:136–148.
7. Carrillo MA, Hallem EA (2015) Gas sensing in nematodes. *Mol Neurobiol* 51:919–931.
8. Brandt JP, Ringstad N (2015) Toll-like receptor signaling promotes development and function of sensory neurons required for a *C. elegans* pathogen-avoidance behavior. *Curr Biol* 25:2228–2237.
9. Hallem EA, Sternberg PW (2008) Acute carbon dioxide avoidance in *Caenorhabditis elegans*. *Proc Natl Acad Sci USA* 105:8038–8043.
10. Bretscher AJ, Busch KE, de Bono M (2008) A carbon dioxide avoidance behavior is integrated with responses to ambient oxygen and food in *Caenorhabditis elegans*. *Proc Natl Acad Sci USA* 105:8044–8049.
11. Bretscher AJ, et al. (2011) Temperature, oxygen, and salt-sensing neurons in *C. elegans* are carbon dioxide sensors that control avoidance behavior. *Neuron* 69: 1099–1113.
12. Carrillo MA, Guillermin ML, Rengarajan S, Okubo RP, Hallem EA (2013) O_2-sensing neurons control CO_2 response in *C. elegans*. *J Neurosci* 33:9675–9683.
13. Kodama-Namba E, et al. (2013) Cross-modulation of homeostatic responses to temperature, oxygen and carbon dioxide in *C. elegans*. *PLoS Genet* 9:e1004011.
14. Guillermin ML, Carrillo MA, Hallem EA (2017) A single set of interneurons drives opposite behaviors in *C. elegans*. *Curr Biol* 27:2630–2639.
15. Fenk LA, de Bono M (2017) Memory of recent oxygen experience switches pheromone valence in *Caenorhabditis elegans*. *Proc Natl Acad Sci USA* 114:4195–4200.
16. Hallem EA, et al. (2011) Receptor-type guanylate cyclase is required for carbon dioxide sensation by *Caenorhabditis elegans*. *Proc Natl Acad Sci USA* 108:254–259.
17. Smith ES, Martinez-Velazquez L, Ringstad N (2013) A chemoreceptor that detects molecular carbon dioxide. *J Biol Chem* 288:37071–37081.
18. Fenk LA, de Bono M (2015) Environmental CO_2 inhibits *Caenorhabditis elegans* egg-laying by modulating olfactory neurons and evokes widespread changes in neural activity. *Proc Natl Acad Sci USA* 112:E3525–E3534.
19. Tsalik EL, Hobert O (2003) Functional mapping of neurons that control locomotory behavior in *Caenorhabditis elegans*. *J Neurobiol* 56:178–197.
20. Gray JM, Hill JJ, Bargmann CI (2005) A circuit for navigation in *Caenorhabditis elegans*. *Proc Natl Acad Sci USA* 102:3184–3191.
21. Chase DL, Koelle MR (2007) Biogenic amine neurotransmitters in *C. elegans*. *WormBook*, pp 1–15. Available at www.wormbook.org. Accessed December 1, 2018.
22. Hills T, Brockie PJ, Maricq AV (2004) Dopamine and glutamate control area-restricted search behavior in *Caenorhabditis elegans*. *J Neurosci* 24:1217–1225.
23. Jayanthi LD, et al. (1998) The *Caenorhabditis elegans* gene T23G5.5 encodes an antidepressant- and cocaine-sensitive dopamine transporter. *Mol Pharmacol* 54:601–609.
24. Ringstad N, Abe N, Horvitz HR (2009) Ligand-gated chloride channels are receptors for biogenic amines in *C. elegans*. *Science* 325:96–100.
25. Roeder T (2005) Tyramine and octopamine: Ruling behavior and metabolism. *Annu Rev Entomol* 50:447–477.
26. Jin X, Pokala N, Bargmann CI (2016) Distinct circuits for the formation and retrieval of an imprinted olfactory memory. *Cell* 164:632–643.
27. Pokala N, Liu Q, Gordus A, Bargmann CI (2014) Inducible and titratable silencing of *Caenorhabditis elegans* neurons *in vivo* with histamine-gated chloride channels. *Proc Natl Acad Sci USA* 111:2770–2775.
28. Noble T, Stieglitz J, Srinivasan S (2013) An integrated serotonin and octopamine neuronal circuit directs the release of an endocrine signal to control *C. elegans* body fat. *Cell Metab* 18:672–684.
29. Yoshida M, Oami E, Wang M, Ishiura S, Suo S (2014) Nonredundant function of two highly homologous octopamine receptors in food-deprivation-mediated signaling in *Caenorhabditis elegans*. *J Neurosci Res* 92:671–678.
30. Félix MA, Duveau F (2012) Population dynamics and habitat sharing of natural populations of *Caenorhabditis elegans* and *C. briggsae*. *BMC Biol* 10:59.
31. Beier S, Bolley M, Traunspurger W (2004) Predator–prey interactions between *Dugesia gonocephala* and free-living nematodes. *Freshw Biol* 49:77–86.
32. Wilecki M, Lightfoot JW, Susoy V, Sommer RJ (2015) Predatory feeding behaviour in *Pristionchus* nematodes is dependent on phenotypic plasticity and induced by serotonin. *J Exp Biol* 218:1306–1313.
33. Padilla SL, et al. (2016) Agouti-related peptide neural circuits mediate adaptive behaviors in the starved state. *Nat Neurosci* 19:734–741.
34. Symmonds M, Emmanuel JJ, Drew ME, Batterham RL, Dolan RJ (2010) Metabolic state alters economic decision making under risk in humans. *PLoS One* 5:e11090.
35. Damsgard B, Dill LM (1998) Risk-taking behavior in weight-compensating coho salmon, *Oncorhynchus kisutch*. *Behav Ecol* 9:26–32.
36. Thomson JS, Watts PC, Pottinger TG, Sneddon LU (2012) Plasticity of boldness in rainbow trout, *Oncorhynchus mykiss*: Do hunger and predation influence risk-taking behaviour? *Horm Behav* 61:750–757.
37. Heithaus MR, et al. (2007) State-dependent risk-taking by green sea turtles mediates top-down effects of tiger shark intimidation in a marine ecosystem. *J Anim Ecol* 76: 837–844.
38. Hawk JD, et al. (2018) Integration of plasticity mechanisms within a single sensory neuron of *C. elegans* actuates a memory. *Neuron* 97:356–367.